Recent N* Results from Pion Electroproduction with CLAS

Kyungseon Joo

University of Connecticut, Storrs, CT 06269, U.S.A.

Abstract. Pion electroproduction in the resonance region has been studied as a means of exploring the physics underlying the structure of the nucleon. An extensive program with the CEBAF large acceptance spectrometer (CLAS) at Jefferson Lab, is currently underway to study electromagnetic transition form factors of nucleon low-lying excitation states and their dependence on the distance scale through pseudoscaler meson electroproduction, which we discuss in this report.

Keywords: QCD, Nucleon excitation, Electromagnetic scattering
PACS: 12.38.-t, 13.60.-r

INTRODUCTION

One of the fundamental questions in hadronic physics is "What is the structure of the nucleon?" We have learned that when probing the nucleon at short distances, the quarks and gluons of QCD are the fundamental degrees of freedom. At large distances, the answer is much less clear. This is, in part, due to the complexity of solving QCD in this regime and in part, due to the lack of relevant experimental information. An extensive program with the CEBAF large acceptance spectrometer (CLAS) at Jefferson Lab, is currently underway to provide answers to this basic question of hadronic physics by studying electromagnetic transition form factors of nucleon low-lying excitation states and their dependence on the distance scale through pseudoscaler meson electroproduction (π^0, π^+ and η channels) on protons for excitation energies up to 2 GeV. We discuss recent developments in the study of the transition amplitudes of $\gamma^* N \to \Delta(1232)$ and $\gamma^* N \to P_{11}(1440)$ through pion electroproduction on protons.

POLARIZED (5TH) STRUCTURE FUNCTION $\sigma_{LT'}$

We begin with our recent advancement in the beam spin asymmetry measurements to access the 5-th structure function $\sigma_{LT'}$ in the $\Delta(1232)$ resonance [1, 2] and the second resonance regions [3]. $\sigma_{LT'}$ measures the imaginary part of the interference of longitudinal and transverse amplitudes:

$$\sigma_{LT'} \propto Im(L^* T) = Im(L)Re(T) - Re(L)Im(T) \tag{1}$$

where L and T represent the longitudinal and transverse amplitude, respectively.

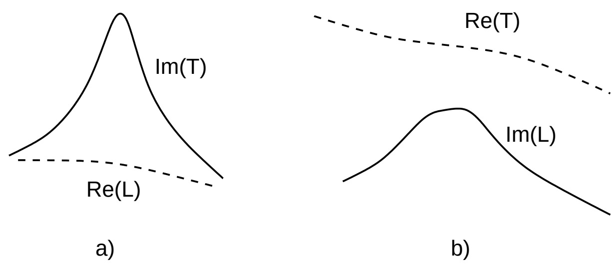

FIGURE 1. Illustration of sensitivity of $\sigma_{LT'}$ to different physics. a) Weak background $Re(L)$ buried under strong resonance $Im(T)$. b) Weak resonance $Im(L)$ buried under strong background $Re(T)$. In each case interference through Equation 1 allows the stronger amplitude to amplify the weaker amplitude, making the latter experimentally accessible.

Important information about multipole phases is available through this observable, which is important above the 2π threshold where unitarity constraints from Watson's Theorem no longer apply. Coupled channel calculations of resonance decays develop sign ambiguities which can be partially resolved using phase information. In addition, $\sigma_{LT'}$ can serve to amplify pion Born terms or other sources of non-resonant backgrounds, or to increase sensitivity to weak resonances such as Roper, as illustrated in Figure 1.

As shown in Figure 2, recent measurements of $\sigma_{LT'}$ in the $\Delta(1232)$ region [1, 2] indicate that largely real non-resonant multipoles are greatly amplified by the imaginary part of the dominant and well-determined M_{1+} resonant multipole as shown schematically in Figure 1 (a). In particular our measurement of the $\sigma_{LT'}(\pi^+n)$ channel (Figure 2 (bottom)) was well described by several phenomenological unitary models, indicating that the dominant t-channel pion pole and Born terms are under control.

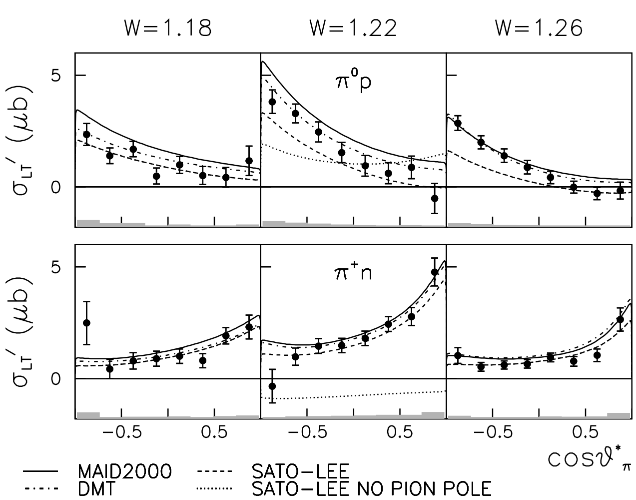

FIGURE 2. CLAS measurements of $\sigma_{LT'}$ versus $\cos\theta^*_\pi$ for the $\pi^0 p$ channel [1] (top) and for the π^+n channel [2] (bottom) extracted at Q^2=0.40 GeV^2 and $W = 1.18 - 1.26$ GeV. The curves show model predictions. The error bars are statistical and the shaded bars at the bottom of the figures show estimated systematic errors.

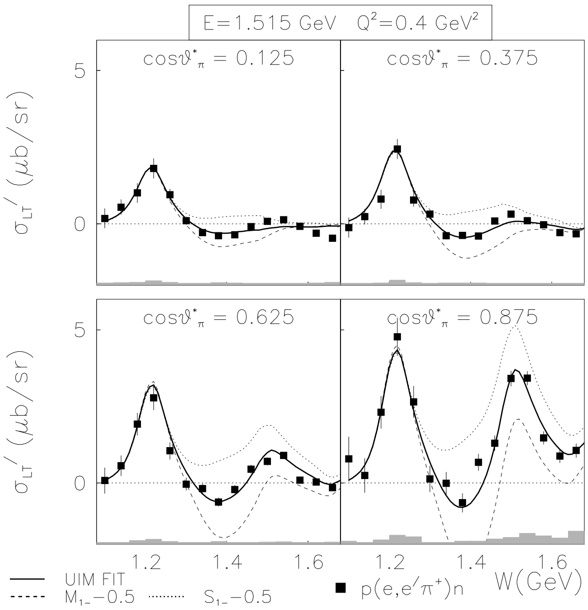

FIGURE 3. CLAS measurements of $\sigma_{LT'}$ versus W (GeV) for the π^+n channel extracted at Q^2=0.40 GeV^2 for different $\cos\theta_\pi^*$ points. The solid line shows the best fit using the Unitary Isobar Model of Aznauryan [4]. The sensitivity of $\sigma_{LT'}$ to the Roper resonance is demonstrated by the dashed and dotted curves where the Roper contributions to M_{1-} and S_{1-} are shifted by $-0.5\ \mu b^{1/2}$. The error bars are statistical and the shaded bars at the bottom of the figures show estimated systematic errors.

These contributions determine the real parts of the dominant non-resonant multipoles in the Roper resonance region and under the conditions illustrated in Figure 1 (b), the small Roper resonant multipoles, which are largely imaginary, can be greatly amplified by the well-determined non-resonant multipoles. The significance of this interference is illustrated in Figure 3, which shows the W dependence of $\sigma_{LT'}(\pi^+n)$ at $Q^2 = 0.4$ GeV^2 for different $\cos\theta_\pi^*$ bins, compared with the unitary isobar model (UIM) [4] developed at JLab. Figure 3 also shows the result of the UIM calculation after shifting the resonant part of each Roper multipole M_{1-} and S_{1-} by $-0.5\ \mu b^{1/2}$, leaving the other at the fitted value. This shift was comparable to the final fitted value of S_{1-}. It clearly shows that the sensitivity is larger in the W region where the imaginary part of the Roper multipoles is nonzero, and maximized in the forward direction due to the interference through the pion pole term.

THE $\gamma^*N \to \Delta(1232)$ TRANSITION FORM FACTORS

The first results [5] was published for the $N \to \Delta(1232)$ transition from CLAS data in the Q^2 range of 0.4 – 1.8 GeV^2 in 2002. The new results in the Q^2 range of 3.0 – 6.0 GeV^2 were recently published in Phys. Rev. Lett [6]. With extensive coverage over angles and energies and polarization observables, the pion electroproduction data from CLAS have allowed nearly model-independent determinations of $\gamma^*N \to \Delta(1232)$ transition form

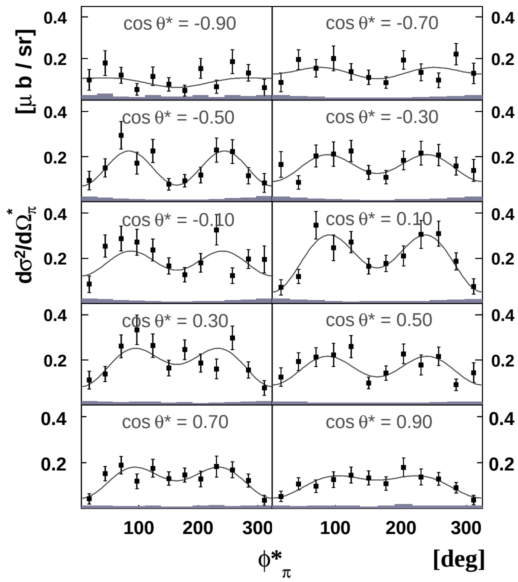

FIGURE 4. The extracted differential cross section of $\gamma^* p \to p\pi^0$ as a function of ϕ^*_π for each $\cos(\theta^*_\pi)$ bin in the center-of-mass system at W=1.25 GeV^2 and Q^2=4.2 GeV^2. The error bars are statistical, and the gray band at the bottom of each panel corresponds to the systematic. The solid curves represent the fit using UIM [4].

factors. Typical differential cross sections in $p\pi^0$ center-of-mass system are shown in Figure 4 for invariant energy W near the $\Delta(1232)$ peak.

In order to extract the $\Delta(1232)$ multipoles M_{1+}, E_{1+} and S_{1+}, the unitary isobar model (UIM) [4], developed at JLab, was used. This model incorporates the isobar approach as in Reference [8]. The non-resonant background consists of the Born term and the t-channel ρ and ω contributions. To calculate the Born term the latest available measurements of the nucleon and pion form factors are used. Underlying tails from resonances such as the $P_{11}(1440)$, $D_{13}(1520)$ and $S_{11}(1535)$, which are modeled as Breit–Wigner shapes, are also incorporated. The contributions of these resonances are evaluated according to information known from world data and the latest CLAS measurements. The dependence of the extracted results on uncertainties due to the non-resonant and higher resonance contributions is included in the systematic errors.

Figure 5(a) shows the extracted amplitude ratios $R_{EM} = E_{1+}/M_{1+}$ and $R_{SM} = S_{1+}/M_{1+}$. It can be seen that R_{EM} is small and negative over the entire Q^2 range, indicating strong helicity non-conservation while R_{SM} is negative and its magnitude increases as a function of Q^2. Our results suggest that the region of Q^2 where pQCD processes would be expected to be valid is higher than currently accessible. Adding to the controversy, Reference [9] has suggested that pQCD can possibly be invoked without strict helicity conservation if orbital angular momentum flips are included into the perturbative reaction mechanism. The prediction for R_{SM} of Reference [9] is shown in Figure 5(a) (lower panel). Figure 5(b) shows the extracted $G^*_M/3G_D$ ratio as a function of Q^2 where G^*_M is the $N \to \Delta$ form factor and $G_D = (1+Q^2/0.71)^{-2}$. The most notable feature is that G^*_M decreases with Q^2 faster than the elastic magnetic

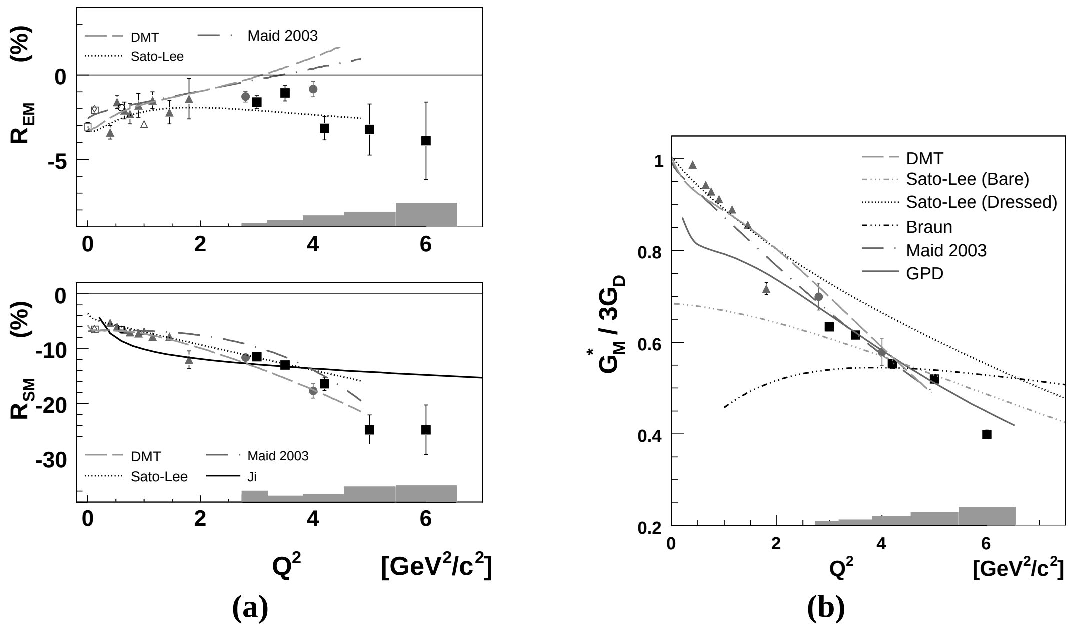

FIGURE 5. (a) Upper panel: the electric quadrupole amplitude relative to the magnetic dipole amplitude, $R_{EM} = E_{1+}/M_{1+}$. Bottom panel: the scaler amplitude relative to the magnetic dipole amplitude, $R_{SM} = S_{1+}/M_{1+}$. (b) The $N \to \Delta$ form factor $G^*_M/3G_D$. The errors shown are statistical, while estimated systematic errors are shown as gray bars at the bottom of the graph.

form factor. This is consistent with Reference [10], which pointed out that, through the application of chiral symmetry, G^*_M can be directly related to the isovector part of the nucleon elastic form factors. This idea was applied in the framework of Generalized Parton Distributions (GPDs) by Reference [11], and later by Reference [12], to suggest that the falloff of G^*_M is related to the falloff of G^p_E [13] through their common isovector form factor.

THE $\gamma^* N \to P_{11}(1440)$ TRANSITION FORM FACTORS

For the first time the amplitudes for the Roper resonance have been determined from pion electroproduction of both π^0 and π^+ channels. Especially, new results of the beam spin asymmetry measurements show a large sensitivity to the Roper amplitudes in the $n\pi^+$ channel through their interference with non-resonant backgrounds [3]. The $N \to P_{11}(1440)$ transition amplitudes $A^p_{1/2}$ and $S^p_{1/2}$ extracted from the global analysis of the UIM calculation [4] are shown in Figure 6, compared to recent quark model calculations of the Roper transition form factors [15, 16, 17, 18]. Also shown is a point at $Q^2 = 1.0$ GeV^2 from a recent Jefferson Lab/Hall A experiment by Laveissiere *et al.* [14] based on a MAID03 analysis of backward angle π^0 electroproduction. All the electroproduction points include model errors, and the plotted CLAS points are the average of UIM and dispersion relation fits [4]. The experimental result of a non-zero longitudinal coupling of the Roper appears to rule out the gluonic hybrid model [15] that

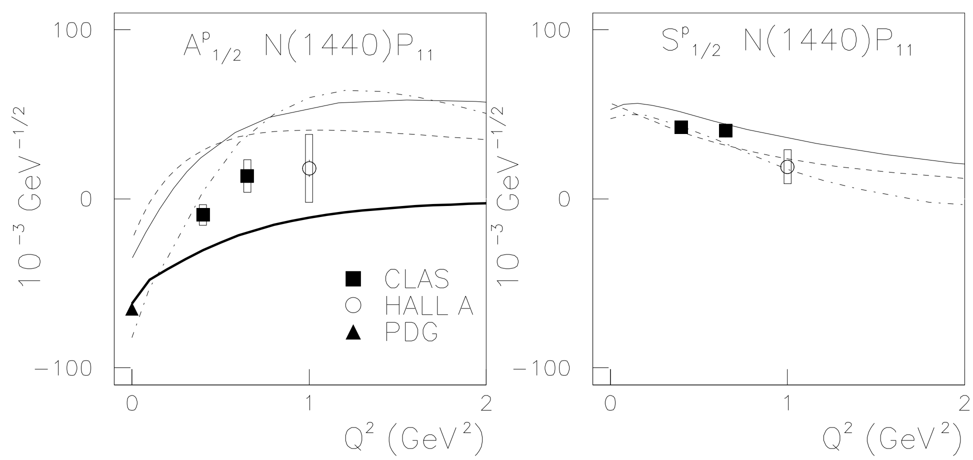

FIGURE 6. Summary of recent measurements showing the Q^2 dependence of the $P_{11}(1440)$ photocoupling amplitudes $A^p_{1/2}$ (left) and $S^p_{1/2}$ (right). The current measurement from CLAS includes model errors arising from the dispersion relations and UIM fits [4]. The data from Hall A [14] show the MAID03 fit model error. Quark model calculations are indicated by bold [15], solid [16], dashed [17] and dot-dashed [18] lines.

predicts the longitudinal amplitude to be identically zero.

SUMMARY

The recent effort of the CLAS collaboration in studying electromagnetic nucleon resonance transition form factors at increasingly short distances has resulted in a strong empirical evidence of large meson contributions to the resonance excitations at large and medium distances. This is particularly evident in the region of the $\gamma^* N\Delta(1232)$ transition where constituent quark models (CQM) are unable to explain the considerably larger strength of the magnetic dipole transition from what is predicted from quark contributions alone [19]. Also, the electric quadrupole transition moment usually expressed through the ratio $R_{EM} = E_{1+}/M_{1+}$ at the resonance pole, is much larger ($R_{EM} \approx 2-4\%$) than the predicted $R^{CQM}_{EM} < 0.5\%$. In the region of the Roper resonance $P_{11}(1440)$, the transverse transition amplitude $A_{1/2}(Q^2)$ shows a strong Q^2 dependence at small photon virtualities, even changing sign in the range $Q^2 = 0.5-1$ GeV^2 [4] as shown in Figure 6 (left). Moreover, the longitudinal transition amplitude $S_{1/2}$ is large at small Q^2, also indicating strong hadronic contributions to the resonance transition strength as shown in Figure 6 (right). This empirical information is best explained by large meson cloud effects. It is also supported by calculations within the chiral quark model [20] that discuss the role of these $q\bar{q}$ components in the wave function of the excited states, as well as of the nucleon.

REFERENCES

1. K. Joo *et al.*, Phys. Rev. **C68**, 033201 (2003).

2. K. Joo *et al.*, Phys. Rev. **C70**, 042201 (2004).
3. K. Joo *et al.*, Phys. Rev. **C72**, 058202 (2005).
4. I. Aznauryan *et al.*, Phys. Rev. **C71**, 015201 (2005).
5. K. Joo *et al.*, Phys. Rev. Lett. **88**, 122001 (2002).
6. M. Ungaro *et al.*, Phys. Rev. Lett. **97**, 112003 (2006).
7. H. Egiyan *et al.*, Phys. Rev. **C72**, 025204 (2006).
8. D. Drechsel, O. Hanstein, S.S. Kamalov and D. Drechsel, Nucl. Phys. **A645**, 145 (1999).
9. X. Ji, J.P. Ma and F. Yuan, Phys. Rev. Lett. **90**, 241601 (2003).
10. K. Goeke, M.V. Polyakov and M. Vanderhaegen, Prog. Part. Nucl. Phys. **47**, 401 (2001).
11. P. Stoler, Phys. Rev. Lett. **91**, 172303 (2003).
12. M. Guidal, M.V. Polyakov, A.V. Radyushkin and M. Vanderhaegen, Phys. Rev. **D72**, 054013 (2005).
13. O. Gayou *et al.*, Phys. Rev. **C64**, 038202 (2001).
14. G. Laveissiere *et al.*, Phys. Rev. **C69**, 045203 (2004).
15. Z. Li, V.D. Burkert and Z. Li, Phys. Rev. **D46**, 70 (1992).
16. S. Capstick and B.D. Keister, Phys. Rev. **D51**, 3598 (1995).
17. S. Simula, Proceedings of the Workshop on The Physics of Excited Nucleons, NSTAR 2001, p.135.
18. F. Cano and P. Gonzalez, Phys. Lett. **B431**, 270 (1998).
19. R.A. Arndt *et al.*, Phys. Rev. **C66**, 055213 (2002).
20. Q.B. Li and D.O. Riska, nucl-th/0605076.